

Rapid Communications

Rapid Communications are intended for the accelerated publication of important new results and are therefore given priority treatment both in the editorial office and in production. A Rapid Communication in Physical Review B should be no longer than 4 printed pages and must be accompanied by an abstract. Page proofs are sent to authors.

Size effects and charge-density-wave pinning in $\text{Nb}_{1-x}\text{Ti}_x\text{Se}_3$: Evidence for weak pinning by a nonisoelectronic impurity

D. A. DiCarlo, J. McCarten, T. L. Adelman, M. Maher, and R. E. Thorne

*Laboratory of Atomic and Solid State Physics and Materials Science Center,
Cornell University, Ithaca, New York 14853-2501*

(Received 22 May 1990)

We report measurements of the threshold electric field E_T for charge-density-wave (CDW) depinning in Ti-doped NbSe_3 . In crystals with large cross-sectional dimensions, E_T varies with the residual resistance ratio r_R as $E_T \propto r_R^{-1.3}$. In small crystals, E_T varies inversely with crystal thickness and r_R . Because of pinning by residual defects, qualitatively different E_T - r_R relations may be obtained for different weak-pinning impurities. We show that the Ti-concentration, crystal-size, and CDW-transition dependence of E_T are consistent with weak CDW pinning and with earlier results for Ta impurities, and indicate a Ti pinning strength roughly 40 times larger than that of Ta.

Above a threshold electric field E_T , charge density waves (CDW's) in NbSe_3 and other quasi-one-dimensional conductors become unpinned and begin to slide, resulting in a variety of unusual transport effects.¹ Phase-dependent CDW interaction with impurities is assumed to be the origin of CDW pinning, but the detailed character of this interaction is still poorly understood.

Two types of pinning are distinguished: (i) strong pinning, in which the CDW phase is pinned at each impurity site,²⁻⁴ and (ii) weak pinning, in which the CDW phase is pinned on lengths L much greater than the average impurity spacing by fluctuations in the impurity potential.² The threshold field E_T provides the most easily quantified manifestation of the CDW-impurity interaction. For weak impurities, E_T is predicted to vary with the square of the impurity concentration n_i , $E_T \propto n_i^2$, while for strong impurities, $E_T \propto n_i$. In NbSe_3 , isoelectronic substitutional impurities such as Ta are expected to pin weakly, although previous Ta doping studies^{5,6} have yielded ambiguous results.

Recently, we have shown⁷ that the dependence of E_T on crystal cross-sectional dimensions reported by Borodin *et al.*⁸ and by Yetman and Gill⁹ must be accounted for when studying the effects of impurities. For Ta impurities, we find that E_T varies with the residual resistance ratio (r_R), proportional to the Ta concentration n_i , as $E_T \propto r_R^{-2}$ in large NbSe_3 crystals. In small crystals, E_T varies linearly with Ta concentration and inversely with crystal thickness. These results are consistent with weak CDW pinning in three and two dimensions, respectively, suggesting that size dependence of E_T occurs when the transverse crystal dimensions become comparable to the transverse CDW phase-phase correlation length.

The initial objective of this study was to investigate strong pinning of CDW's in NbSe_3 . Ti was chosen for the dopant because it is expected to form a charged and therefore strongly pinning defect, because it transports easily during crystal growth, because it forms a selenide similar to NbSe_3 , and thus is likely to form only point defects, and because previous studies^{5,10-12} indicated that Ti pins the CDW more strongly than Ta with $E_T \propto r_R^{-1}$ (Ref. 10).

Here we show that E_T in Ti-doped NbSe_3 crystals exhibits a crystal size dependence similar to that observed with Ta doping. By accounting for CDW pinning by defects other than Ti atoms, we show that both the E_T - r_R relation measured in large crystals and the size dependence observed in small crystals are consistent with weak pinning, and with our earlier results for Ta impurities these results provide strong additional evidence for the weak-pinning dimensionality crossover interpretation of the size effects.

NbSe_3 single crystals containing nominal Ti concentrations n_i between 0.003 and 1.1 at.% were prepared from the elements by vapor transport growth. The smallest Ti doping levels were achieved by reacting Nb, Se, and Ti to form $\text{Nb}_{1-x}\text{Ti}_x\text{Se}_3$ powder, and then reacting small amounts of this powder with additional Nb and Se. The Ti content of heavily doped crystals (0.07 and 1.1 at.% Ti) was determined using proton-induced x-ray emission spectroscopy and atomic absorption spectroscopy, and was approximately equal to that expected from the Ti fraction in the source materials, indicating comparable transport rates for Ti and Nb. These chemical analysis methods could not be used to accurately determine Ti concentrations in more lightly doped crystals. The Ti concentration n_i was instead characterized using the residual resistance

ratio $r_R = R(300 \text{ K})/R(4.2 \text{ K})$.¹³ In large crystals, r_R is independent of crystal size⁷ and

$$r_R^{-1} = r_{R_0}^{-1} + b_i^{-1} n_i, \quad (1)$$

where r_{R_0} is the contribution from the residual defects, and b_i depends upon the impurity type.⁵ From the Ti content of the source materials and the measured r_R , $b_{\text{Ti}} \approx 1 \times 10^{19} \text{ cm}^{-3}$, a factor of 20 smaller than for Ta impurities, consistent with the much more strongly perturbing character expected for Ti.

NbSe₃ crystals grow as ribbonlike whiskers with typical lengths (along the highly conducting b axis) of several millimeters, widths of 1–1000 μm , and thicknesses 1–2 orders of magnitude smaller than the width. The length and extremal width of each crystal were measured using an optical microscope, and the average thickness calculated from these dimensions and the measured room-temperature resistance, assuming $\sigma(300 \text{ K}) = 5.4 \times 10^3 \Omega^{-1} \text{ cm}^{-1}$ (Ref. 14). The threshold field E_T was measured using a standard four-probe configuration, with contacts formed using silver paint. In undoped NbSe₃, the threshold field is strongly temperature dependent, and the temperature dependence depends strongly upon crystal cross-sectional dimensions for $90 \text{ K} < T < 130 \text{ K}$.¹⁵ Most of the present measurements were thus performed at $T = 77 \text{ K}$. For large NbSe₃ crystals with no added Ti, prepared using identical procedures and source materials as for Ti-doped crystals, $r_{R_0} \approx 120$ and $E_{T_0}(T = 77 \text{ K}) \approx 90 \text{ mV/cm}$.

Figure 1 shows the threshold electric field E_T at $T = 77 \text{ K}$ versus average crystal thickness t , for crystals from five growths having Ti concentrations of up to 0.014 at.%. As with Ta impurities, two regimes are observed: a bulk regime in which E_T is independent of crystal thickness, and a size-dependent regime in which E_T increases with de-

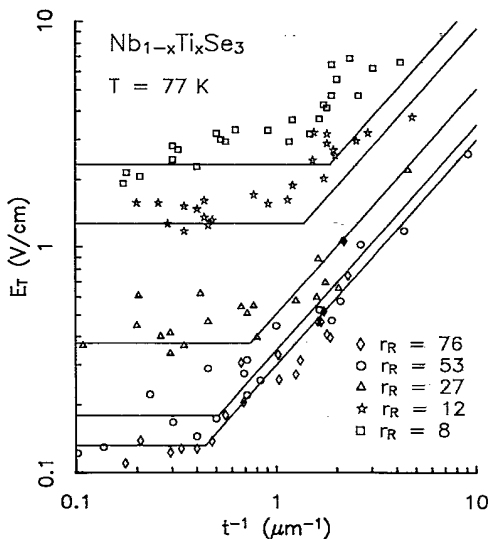


FIG. 1. Threshold electric field E_T at $T = 77 \text{ K}$ vs inverse crystal thickness for NbSe₃ crystals from five growths with different Ti concentrations. The r_R values represent averages for crystals with large cross sections. The solid lines represent the weak pinning fits discussed in the text.

creasing thickness. The thickness is the relevant dimension controlling the size effects because the cross-sectional aspect ratio of typical crystals is considerably larger than the electronic anisotropy; for crystals of a given thickness t , E_T shows little dependence on crystal width w down to $w \approx 2t$. Considerable scatter in the size-dependent regime results because the cross sections of most crystals are highly irregular with several “thicknesses.” The maximum thickness, which may deviate from the average thickness by a factor of 2 or more, can often determine the measured E_T , depending upon the cross-section geometry and upon the presence of dislocations or cracks running along the whisker axis. Also, in the smallest crystals $w \approx t$, so that contributions to E_T from finite crystal width may also become significant.

A least-squares fit to threshold field E_T vs r_R data for crystals from the bulk or size-independent regime in Fig. 1 yields

$$E_T = [(3.0 \pm 0.5) \times 10] r_R^{-c} \text{ V/cm}, \quad c = 1.35 \pm 0.1. \quad (2)$$

The observed exponent differs from both the weak and strong pinning predictions, although it is fairly close to $\frac{4}{3}$, as predicted in an alternative model⁴ of strong pinning. However, our NbSe₃ crystals contain a variety of defects other than Ti impurities, and these other defects must contribute to the measured E_T - r_R relation. The residual pinning is due primarily to an ~ 100 ppm concentration of Ta impurities, which are present in the Nb source material; concentrations of other defects are much smaller. The residual pinning is thus expected to be weak.⁷ If the intentionally added impurities also pin weakly, standard random-walk arguments predict a threshold field

$$\sqrt{E_T} = \sqrt{E_{T_0}} + a_i n_i, \quad (3)$$

where E_{T_0} is the threshold field due to residual pinning. If both the added impurities and the residual defects pin strongly, the pinning energies add and

$$E_T = E_{T_0} + a_i n_i. \quad (4)$$

This expression is expected to be approximately valid in the case of weak residual pinning, with the greatest uncertainties in the regime where the residual and n_i -related pinning strengths are comparable. Substituting for n_i using Eq. (1) yields

$$\sqrt{E_T} = (\sqrt{E_{T_0}} - a_i b_i r_{R_0}^{-1}) + a_i b_i r_R^{-1} \quad (5)$$

for weak pinning and

$$E_T = (E_{T_0} - a_i b_i r_{R_0}^{-1}) + a_i b_i r_R^{-1} \quad (6)$$

for strong pinning.

Figure 2 plots E_T vs r_R^{-1} for crystals from the size-independent regime, together with best fits to Eqs. (5) and (6). The weak pinning fit is somewhat better, although not convincingly so. However, these fits were made without constraints, i.e., all constants were assumed adjustable. If the fits are required to pass through (r_{R_0}, E_{T_0}) , the weak pinning fit is essentially unchanged while the strong pinning fit becomes much worse. Figure 3 compares data and unconstrained weak pinning fits for Ti- and

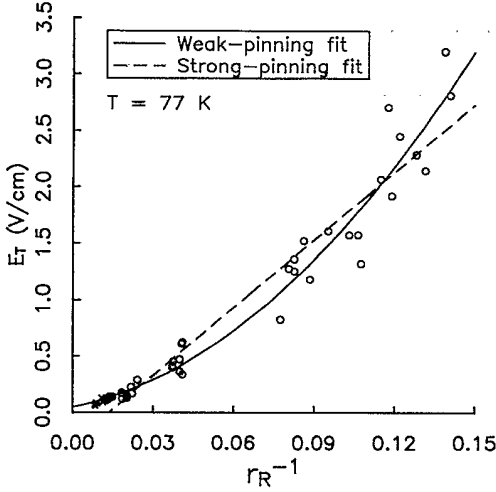


FIG. 2. Threshold electric field E_T at 77 K vs r_R^{-1} for Ti-doped crystals from the size-independent regime. The solid and dashed lines represent the weak and strong pinning fits provided by Eqs. (5) and (6), respectively. Crosses represent values for undoped crystals.

Ta-doped NbSe₃. The fits intersect at the measured E_{T_0} and r_{R_0} . The slopes of these fits differ by a factor of 3; for a given r_R , E_T for Ta doping is much larger than for Ti doping. However, for a given impurity concentration n_i , r_R for Ta is much smaller, so that E_T for Ti is approximately 40 times larger than for Ta.¹⁶ In the revised view of strong pinning given in Ref 4, no strong dependence of E_T on impurity type is expected, in clear disagreement with experiment. In three-dimensional (3D) weak pinning,²

$$E_T^{(3D)} = \left[\frac{27}{\pi^3} \frac{\xi_z^4}{\xi_x^2 \xi_y^2} \frac{(v\rho_1 A_0)^4}{e(\hbar v_F)^3} \right] n_i^2, \quad (7)$$

where v is the impurity potential, ρ_1 is the amplitude of

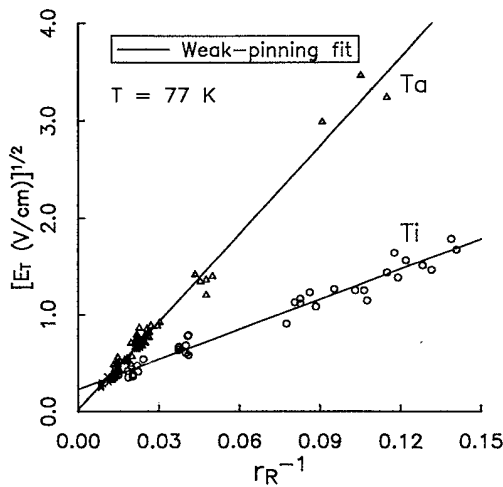


FIG. 3. Comparison of $T=77$ K E_T - r_R^{-1} data for Ta- and Ti-doped NbSe₃ crystals in the size-independent regime. The solid lines represent the weak pinning fits provided by Eq. (5). Crosses represent values for undoped crystals.

the CDW charge modulation, A_0 is the cross-sectional area per chain, v_F is the Fermi velocity, ξ is the amplitude coherence length, and z is along the direction of CDW motion. The threshold ratio thus implies that $v\rho_1(\text{Ti}) \approx 2.5v\rho_1(\text{Ta})$, considerably smaller than has been expected.

We have also measured the temperature dependence of E_T for the two CDW's which form below $T_{p1} = 145$ K and $T_{p2} = 59$ K in NbSe₃. For a given Ti concentration, the ratio of the minimum bulk thresholds $E_{T_1}^{\text{min}}/E_{T_2}^{\text{min}} \approx 7-8$, comparable to the ratio of 8-9 obtained with Ta impurities.^{15,17} In strong pinning,^{2,4} $E_{T_1}/E_{T_2} \approx \Delta_1/\Delta_2 \approx 2.5$.¹⁸ In weak pinning, the threshold ratio is very sensitive to v_F , ρ_1 , and the effective A_0 , whose values are imprecisely known.

If Ti and Ta both act as weak pinning centers in NbSe₃, then why do power law fits to E_T - r_R^{-1} data for large crystals yield exponents—1.9 for Ta vs 1.3 for Ti—which are so different? In the presence of residual weak pinning, the slope of a $\log(E_T)$ vs $\log(r_R^{-1})$ plot is expected to be

$$c = \frac{\partial \log(E_T)}{\partial \log(r_R^{-1})} \approx 2 - 2[(\sqrt{E_{T_0}} - a_{i_0} b_i r_{R_0}^{-1})/\sqrt{E_T}] \quad (8)$$

and will be close to two only if $(\sqrt{E_{T_0}} - a_{i_0} b_i r_{R_0}^{-1})$, which corresponds to the y intercept in the fits of Fig. 3, is small. This intercept is negligible for Ta but quite large for Ti. The power-law exponents for Ti and Ta thus differ because Ti has a relatively much larger effect on r_R than on E_T .

To account for the size dependence of E_T , we extend our earlier weak pinning analysis, which has been shown to be consistent with very similar size effects observed in Ta-doped crystals. A crossover from 3D to 2D weak pinning is expected in ribbonlike NbSe₃ crystals when the crystal thickness t becomes comparable to the transverse CDW phase-phase correlation length L_x . In 2D weak pinning,

$$E_T^{(2D)} = \left[\frac{4}{\pi} \frac{(v\rho_1 A_0)^2}{e\hbar v_F} \frac{\xi_z}{\xi_x} \right] \frac{n_i}{t} \quad (9)$$

and varies linearly with impurity concentration and inversely with the constrained dimension t . The ratio

$$\frac{(E_T^{(2D)} t)^2}{E_T^{(3D)}} = \frac{16}{27} \frac{\pi \hbar v_F}{e} \frac{\xi_y^2}{\xi_z^2} \quad (10)$$

is independent of impurity type and concentration. Thus, using the weak pinning fit in Fig. 3 to the bulk threshold $E_T^{(3D)}$ and the ratio $(E_T^{(2D)} t)^2/E_T^{(3D)} = 6.7 \times 10^{-9}$ V cm, obtained by fitting data for Ta-doped crystals, the size dependence of E_T in Ti-doped crystals can be predicted *with no adjustable parameters*. This prediction is indicated by the solid lines in Fig. 1. Although scatter in the data is considerable, the overall qualitative and quantitative agreement is remarkably good, providing strong additional evidence for the weak pinning dimensionality crossover interpretation of the size effects.

Other interpretations of the size dependence of E_T have been proposed. Simple surface pinning models, in which the CDW is pinned by defects at the crystal surface,

drastically underestimate the size dependence of E_T in doped crystals. In a surface pinning model proposed by Gill,⁹ the CDW near the surface adjusts its wave vector towards the commensurate value and becomes strongly pinned. CDW sliding then occurs when the more weakly pinned bulk CDW shears by glide of edge dislocations from the strongly pinned surface CDW. While this model might plausibly reproduce some of the observed behavior (for example, the size dependence might be enhanced in doped crystals if the dislocations are pinned to the impurities), there is no direct evidence for surface CDW commensurability or for the importance of edge dislocations in micron-thick crystals, nor do we find any evidence suggesting that CDW pinning in small crystals is fundamentally different from that in large crystals. And unlike the weak pinning model, performing quantitative comparisons with experiment would seem extremely difficult.

The establishment of Ti as a weak pinning impurity raises questions regarding the observability of strong CDW pinning by isolated impurities in NbSe₃. Relatively minute Ti concentrations (5–50 ppm by weight) produce very large threshold fields. Comparable concentrations of strongly pinning impurities thus would likely yield threshold fields which, because of Ohmic heating, are too large

to measure; and much smaller concentrations would be extremely difficult to quantify. In addition, impurities more strongly perturbing than Ti are unlikely to be simply substitutional, and may produce extended defects whose pinning character is more difficult to analyze. (The isolated phase-slip centers¹⁹ produce by Fe doping may be an example of this.)

In summary, we have shown that the impurity concentration and CDW transition dependence of E_T in large Ti-doped NbSe₃ crystals are consistent with weak pinning. The crystal size dependence of E_T observed in crystals with small cross-sectional dimensions is consistent with a crossover from 3D to 2D weak pinning. Together with results for Ta-doped NbSe₃, these results establish pinning dimensionality as an important parameter in the study of sliding CDW systems.

We wish to thank U. Eckern, J. C. Gill, S. Ramakrishna, and John Bardeen for fruitful discussions. Two of us (D.A.D. and M.M.) acknowledge support provided by the National Science Foundation (NSF) and by IBM, respectively. This work was supported by the Alfred P. Sloan Foundation, by the AT&T Foundation, and by NSF Grant No. DMR-89-58515.

¹For comprehensive reviews of CDW's, see *Electronic Properties of Quasi-One-Dimensional Materials*, edited by P. Monceau (Reidel, Dordrecht, 1985); G. Grüner, *Rev. Mod. Phys.* **60**, 1129 (1988).

²H. Fukuyama and P. A. Lee, *Phys. Rev. B* **17**, 535 (1978); P. A. Lee and T. M. Rice, *ibid.* **19**, 3970 (1979).

³S. Abe, *J. Phys. Soc. Jpn.* **54**, 3494 (1985); **55**, 1987 (1986).

⁴J. R. Tucker, W. G. Lyons, and G. Gammie, *Phys. Rev. B* **38**, 1148 (1988); **40**, 5447 (1989).

⁵J. W. Brill, N. P. Ong, J. C. Eckert, J. W. Savage, S. K. Khanana, and R. B. Somoano, *Phys. Rev. B* **23**, 1517 (1981).

⁶M. Underweiser, M. Maki, B. Alavi, and G. Grüner, *Solid State Commun.* **64**, 181 (1987).

⁷J. McCarten, M. Maher, T. L. Adelman, and R. E. Thorne, *Phys. Rev. Lett.* **63**, 2841 (1989).

⁸D. V. Borodin, F. Ya. Nad', S. Savitskaja, and S. V. Zaitsev-Zotov, *Physica* **143B**, 73 (1986).

⁹P. J. Yetman and J. C. Gill, *Solid State Commun.* **62**, 201 (1987).

¹⁰P. M. Chaikin, W. W. Fuller, R. Laco, J. F. Kwak, R. L. Greene, J. C. Eckert, and N. P. Ong, *Solid State Commun.*

39, 553 (1981).

¹¹P. Monceau, *Physica* **109-110B**, 1890 (1982).

¹²M. Ido, Y. Okajima, H. Wakimoto, and M. Oda, *Physica* **143B**, 54 (1986).

¹³Ohmic conduction in NbSe₃ at low temperatures is by carriers on unnested portions of the Fermi surface.

¹⁴T. L. Adelman, J. McCarten, M. Maher, D. A. DiCarlo, and R. E. Thorne (unpublished); J. Richard (private communication).

¹⁵J. McCarten, D. A. DiCarlo, M. Maher, T. L. Adelman, and R. E. Thorne (unpublished).

¹⁶This ratio is uncertain by roughly a factor of 4, due to a factor of 2 uncertainty in the produce $n_i r_R$ for Ti.

¹⁷These E_T ratios are much larger than reported in previous doping studies (8 vs, e.g., 3 in Ref. 6). Previous studies ignored the size dependence of E_T , which is much larger for $T < T_{p2}$ than for $T_{p2} < T < T_{p1}$.

¹⁸T. Ekino and J. Akimitsu, *Jpn. J. Appl. Phys. Pt. 1* **26**, 625 (1987).

¹⁹R. P. Hall, M. F. Hundley, and A. Zettl, *Phys. Rev. Lett.* **56**, 2399 (1986).